Efficient structural reliability analysis via a weak-intrusive stochastic finite element method

Zhibao Zheng[a,*], Hongzhe Dai[a], Michael Beer[b,c,d]

[a]*School of Civil Engineering, Harbin Institute of Technology, Harbin 150090, China*
[b]*Institute for Risk and Reliability, Leibniz Universität Hannover, Callinstraße 34, 30167 Hannover, Germany*
[c]*Institute for Risk and Uncertainty and School of Engineering, University of Liverpool, Peach Street, Liverpool L69 7ZF, UK*
[d]*International Joint Research Center for Resilient Infrastructure & International Joint Research Center for Engineering Reliability and Stochastic Mechanics, Tongji University, 1239 Siping Road, Shanghai 200092, China*

Abstract

This paper presents a novel methodology for structural reliability analysis by means of the stochastic finite element method (SFEM). The key issue of structural reliability analysis is to determine the limit state function and corresponding multidimensional integral that are usually related to the structural stochastic displacement and/or its derivative, e.g., the stress and strain. In this paper, a novel weak-intrusive SFEM is first used to calculate structural stochastic displacements of all spatial positions. In this method, the stochastic displacement is decoupled into a combination of a series of deterministic displacements with random variable coefficients. An iterative algorithm is then given to solve the deterministic displacements and the corresponding random variables. Based on the stochastic displacement obtained by the SFEM, the limit state function described by the stochastic displacement (and/or its derivative) and the corresponding multidimensional integral encountered in reliability analysis can be calculated in a straightforward way. Failure probabilities of all spatial positions can be obtained at once since the stochastic displacements of all spatial points have been known by using the proposed SFEM. Furthermore, the proposed method can be applied to high-dimensional stochastic problems without any modification. One of the most challenging problems encountered in high-dimensional reliability analysis, known as the curse of dimensionality, can be circumvented with great success. Three numerical examples, including low- and high-dimensional reliability analysis, are given to demonstrate the good accuracy and the high efficiency of the proposed method.

Keywords: Reliability analysis; Stochastic finite element method; Weakly intrusive approximation; Stochastic displacements; Curse of dimensionality;

1. Introduction

As a powerful tool to quantify the uncertainty in practical problems, reliability analysis nowadays has become an indispensable cornerstone for analyzing complex stochastic problems in many fields [1, 2, 3], such as structural design, optimization and decision management. Although significant effort has been made in the modeling and analysis, the estimation of the failure probability in reliability analysis is still challenging [4, 5, 6]. On one hand, since the multidimensional integral encountered in reliability analysis for calculating the failure probability often lies in high-dimensional stochastic spaces (hundreds to more), expensive computational costs for the purpose are usually prohibitive. On the other hand, the limit state surface is rarely known explicitly and only can be evaluated by numerical solutions because the failure region is generally complicated and irregular.

In the past decade, various methods have been developed for the evaluation of multidimensional integrals arising in reliability analysis. The most straightforward method is known as Monte Carlo simulation (MCS). MCS almost converges to the exact value when the number of samples is large enough [7]. In addition, it does not depend on the dimension of stochastic spaces, thus it does not encounter the curse of dimensionality. However, the computational cost for estimating a small failure probability is expensive, which makes this method prohibitive for complex problems in practice. As a robust technique, MCS is usually used to verify the effectiveness of other methods. Some variations have been proposed to improve MCS, such as multi-level MCS, importance sampling, subset simulation, etc [5, 8, 9]. Besides sample-based methods, some non-sampling methods have also been developed for reliability analysis. A typical kind of non-sampling methods for reliability analysis are first/second order reliability method (FORM/SORM) [10, 11]. These methods are based on first/second order series expansion approximation of the failure surface at the so-called design point, then the resulting approximate integral is calculated by asymptotic method.

*Corresponding author
Email address: zhibaozheng@hit.edu.cn (Zhibao Zheng)

These methods generally have good accuracy and efficiency for low-dimensional and weakly nonlinear problems. However, considerable errors may arise in high-dimensional stochastic spaces and nonlinear failure surfaces [12]. Several methods have been proposed to improve the performance of this kind of method [13]. Another popular method used to decrease the computational cost of reliability analysis, known as surrogate model methods, is receiving particular attention and continuously gaining significance. This kind of method calculates a functional surrogate representation as an approximation of the limit state function. The surrogate model is usually constructed in an explicit representation via a set of observed points, then the failure probability can be estimated with cheap computational costs. The constructions of surrogate models are crucial, and available surrogate model methods include response surface method [14, 15, 16], kriging method [17], support vector machine [18], high-dimensional model representation [19], polynomial chaos expansion [20, 21, 22], etc.

In most practical cases, the limit state function in reliability analysis builds a relationship between stochastic spaces of input parameters and the failure probability via the stochastic displacement of the system [20, 23, 24, 25], thus the determination of the stochastic displacement of the system is crucial. For decades, the stochastic finite element method (SFEM), especially the spectral stochastic finite element method and its extensions [26, 27, 28, 29, 30], have received particular attention for solving structural displacements. As an extension of the classical deterministic finite element method to the stochastic framework, the spectral SFEM has been proven efficient both numerically and analytically on numerous stochastic problems in engineering and science [31]. In this kind of method, the unknown stochastic displacement is projected onto a stochastic space spanned by (generalized) polynomial chaos basis. The stochastic Galerkin method is then adopted to transform the original stochastic finite element equation into a deterministic finite element equation, whose size can be up to orders of magnitude larger than the original stochastic problems [26, 27]. However, since extreme computational costs arise as the number of stochastic dimensions and the number of polynomial chaos expansion terms increase, high-resolution solutions of stochastic finite element equations are still a challenge, especially for high-dimensional and large-scale stochastic problems in engineering practice [29, 30].

In this paper, a novel weak-intrusive stochastic finite element method [32] is adopted to solve stochastic displacements of the target systems. In this method, the unknown stochastic displacement is expanded into a summation of the products of a set of deterministic displacements and random variables described in a non-intrusive way, and an iterative algorithm is then given to solve the deterministic displacements and the corresponding random variables one by one. More importantly, the proposed method can be applied to high-dimensional and large-scale stochastic problems with high efficiency, thus it avoids the difficulties of the classical spectral SFEM discussed above. Based on the obtained stochastic displacement, limit state functions and multidimensional integrals in reliability analysis can be calculated in a straightforward way. Failure probabilities of all spatial positions are then calculated using very low computational effort. Furthermore, the failure probability nephogram of the target system can be generated via the failure probabilities of all spatial positions, which opens up a potential way for system reliability analysis and also provides a unified and efficient numerical framework for various reliability analyses.

The paper is organized as follows: Basic problems of reliability analysis are introduced in Section 2. Section 3 gives a novel weak-intrusive stochastic finite element method for determining structural stochastic displacements. Based on the obtained stochastic displacement, a SFEM-based method for reliability analysis is then described in Section 4, followed by the algorithm implementation of the proposed method in Section 5. Three problems are used to demonstrate the performance of the proposed method in Section 6.

2. Structural reliability analysis

Structural reliability analysis is typically described by a scalar limit state function $g(\theta)$ and corresponding failure probability P_f. The evaluation of P_f requires the following multidimensional integral [4, 5]

$$P_f = \int_{g(\theta)\leq 0} f(\theta)\,\mathrm{d}\theta, \tag{1}$$

where $g(\theta) \leq 0$ denotes the failure domain, $f(\theta)$ is the joint probability density function of random variables associated with system parameters and environmental sources. The integral in Eq. (1) for determining the failure probability is usually difficult to evaluate since the limit state surface $g(\theta) = 0$ may have a very complicated geometry and $f(\theta)$ may be defined in high-dimensional stochastic spaces. In most cases, the representation of the limit state function $g(\theta)$ is not known explicitly, thus numerical methods are usually employed for the evaluation of Eq. (1). Existing reliability analysis methods generally evaluate the failure probability at a single point. For general purposes, the spatial limit state function $g(\mathbf{x}, \theta)$ is considered in this paper. Similar to Eq. (1), the spatial failure probability function $P_f(\mathbf{x})$ is defined as

$$P_f(\mathbf{x}) = \int_{g(\mathbf{x},\theta)\leq 0} f(\mathbf{x}, \theta)\, \mathrm{d}\theta, \tag{2}$$

which can also provide an effective way for global reliability analysis for the target system. However, due to the introduction of spatial positions $\mathbf{x}$, the failure probability function $P_f(\mathbf{x})$ in Eq. (2) is more difficult to calculate than that in Eq. (1). Further, Eq. (2) also provides a powerful and unified way for problems with multiple failure modes and unknown design points. Eq. (1) is just considered as a simplified case of Eq. (2) at the design points.

In this paper, we consider the failure probability function $P_f(\mathbf{x})$ of partial differential equation (PDE)-controlled stochastic systems whose displacement is a stochastic function $u(\mathbf{x}, \theta)$. In fact, $g(\mathbf{x}, \theta)$ typically represents a complicated relationship between the inputs and the failure modes via the solution of a potential highly complex stochastic system. Representing the limit state function $g(\mathbf{x}, \theta)$ in the form of the stochastic displacement $u(\mathbf{x}, \theta)$ we have

$$g(\mathbf{x}, \theta) = g\left[h\left(u(\mathbf{x}, \theta)\right), \mathbf{x}, \theta\right], \tag{3}$$

where $h(u(\mathbf{x}, \theta))$ is the function of the stochastic displacement $u(\mathbf{x}, \theta)$. For instance, it can be the stochastic stress, the stochastic strain and the relative stochastic displacement, etc. The $g(u(\mathbf{x}, \theta), \mathbf{x}, \theta)$ represents the displacement-based limit state function when the function $h(u(\mathbf{x}, \theta)) = u(\mathbf{x}, \theta)$. In this way, we approximate the limit state function $g(\mathbf{x}, \theta)$ in an explicit way and the failure probability function $P_f(\mathbf{x})$ is computed efficiently under the known stochastic displacement $u(\mathbf{x}, \theta)$. In the next section, we will introduce an efficient stochastic finite element method to compute the stochastic displacement $u(\mathbf{x}, \theta)$ and then compute Eq. (3) and Eq. (2) based on the obtained solution $u(\mathbf{x}, \theta)$.

3. Stochastic displacements determination using a weak-intrusive SFEM

As an extension of the deterministic finite element method (FEM), SFEM has become a common tool for computing structural stochastic displacements [26, 31]. In the SFEM, system parameters and environmental sources are modeled by use of random variables/fields [33, 34]. By substituting random variables/fields into classical finite element equations, stochastic finite element equations of linear problems can be written as

$$\mathbf{K}(\theta)\,\mathbf{u}(\theta) = \mathbf{F}(\theta), \tag{4}$$

where $\mathbf{K}(\theta) \in \mathbb{R}^{n\times n}$ is the stochastic global stiffness matrix representing stochastic properties of the physical model under investigation, n is the number of degrees of freedom, $\mathbf{u}(\theta) \in \mathbb{R}^n$ is the unknown stochastic displacement and $\mathbf{F}(\theta) \in \mathbb{R}^n$ is the stochastic force vector associated with source terms. It is noted that $\mathbf{u}(\theta)$ in Eq. (4) is a discrete vector form of the original stochastic solution $u(\mathbf{x}, \theta)$ in Eq. (3), which is obtained via the classical finite element discretization. All spatial positions $\mathbf{x}$ are thus embedded into the discrete vector $\mathbf{u}(\theta)$. In the remainder of this paper, we perform the reliability analysis using the stochastic vector $\mathbf{u}(\theta)$ instead of the original stochastic solution $u(\mathbf{x}, \theta)$.

In general, it is a great challenge to compute the high-precision solution of Eq. (4). Spectral stochastic finite element method (SSFEM) is a popular method in the past few decades, in which the stochastic displacement is represented through polynomial chaos expansion (PCE) and Eq. (4) is thus transformed into a deterministic finite element equation by stochastic Galerkin projection [29, 31]. The size of the deterministic finite element equation is much larger than the original stochastic problem and expensive computational costs limit SSFEM to low-dimensional stochastic problems. In order to overcome these difficulties, a novel sample-based SFEM is developed to solve Eq. (4) [32], which represents the unknown stochastic displacement $\mathbf{u}(\theta)$ as

$$\mathbf{u}(\theta) = \sum_{i=1}^{k} \lambda_i(\theta)\,\mathbf{d}_i, \tag{5}$$

where $\{\lambda_i(\theta)\}_{i=1}^k$ and $\{\mathbf{d}_i\}_{i=1}^k$ are unknown random variables and unknown deterministic vectors, respectively. The solution $\mathbf{u}(\theta)$ is approximated after k terms are truncated and the more terms k are retained, the more accurate approximation can be obtained. It is noted that the solution construct of Eq. (5) is independent of the form of Eq. (4), thus it is applicable for both linear and nonlinear stochastic finite element equations. In this paper, we only consider linear stochastic finite element equations and nonlinear problems will be investigated in subsequent studies. Eq. (5) provides a separated form of deterministic and stochastic spaces, which is possible to determine $\{\lambda_i(\theta)\}_{i=1}^k$ and $\{\mathbf{d}_i\}_{i=1}^k$ in their individual spaces, respectively. Hence, one requires to seek deterministic vectors $\{\mathbf{d}_i\}_{i=1}^k$ and corresponding random variables $\{\lambda_i(\theta)\}_{i=1}^k$ such that the approximate solution in Eq. (5) satisfies Eq. (4). In Eq. (5), neither $\{\mathbf{d}_i\}_{i=1}^k$ nor $\{\lambda_i(\theta)\}_{i=1}^k$ are known a priori, we can successively determine these unknown couples $\{\lambda_i(\theta), \mathbf{d}_i\}$ one by one via an iterative process. From this point, we assume that the first $k-1$ terms $\{\lambda_i(\theta), \mathbf{d}_i\}_{i=1}^{k-1}$ have been obtained. In order to compute the couple $\{\lambda_k(\theta), \mathbf{d}_k\}$, substituting Eq. (5) into Eq. (4) yields

$$\mathbf{K}(\theta)\left[\sum_{i=1}^{k-1}\lambda_i(\theta)\,\mathbf{d}_i + \lambda_k(\theta)\,\mathbf{d}_k\right] = \mathbf{F}(\theta). \tag{6}$$

It is not easy to determine $\lambda_k(\theta)$ and $\mathbf{d}_k$ simultaneously. In order to avoid this difficulty, the random variable $\lambda_k(\theta)$ and the vector $\mathbf{d}_k$ are calculated one after another. For the determined random variable $\lambda_k(\theta)$ (or given as an initial value), $\mathbf{d}_k$ can be computed by using stochastic Galerkin method, which corresponds to

$$\mathbb{E}\left\{\lambda_k(\theta)\,\mathbf{K}(\theta)\left[\sum_{i=1}^{k-1}\lambda_i(\theta)\,\mathbf{d}_i + \lambda_k(\theta)\,\mathbf{d}_k\right]\right\} = \mathbb{E}\{\lambda_k(\theta)\,\mathbf{F}(\theta)\}, \tag{7}$$

where $\mathbb{E}\{\cdot\}$ is the expectation operator. Once the vector $\mathbf{d}_k$ has been determined by Eq. (7), the random variable $\lambda_k(\theta)$ can be subsequently computed by applying Galerkin method to Eq. (6), which yields

$$\mathbf{d}_k^{\mathrm{T}}\mathbf{K}(\theta)\left[\sum_{i=1}^{k-1}\lambda_i(\theta)\,\mathbf{d}_i + \lambda_k(\theta)\,\mathbf{d}_k\right] = \mathbf{d}_k^{\mathrm{T}}\mathbf{F}(\theta). \tag{8}$$

In this way, the couple $\{\lambda_k(\theta), \mathbf{d}_k\}$ can be computed by repeatedly solving Eq. (7) and Eq. (8) until they converge to a specified precision. We note that the iterative process of Eq. (7) and Eq. (8) also works for nonlinear stochastic finite element equations, but Eq. (7) and Eq. (8) will be a deterministic nonlinear finite element equation of $\mathbf{d}_k$ and a one-dimensional nonlinear stochastic algebraic equation of $\lambda_k(\theta)$, respectively. For practical implementation, the vector $\mathbf{d}_k$ is unitized as $\mathbf{d}_k^{\mathrm{T}}\mathbf{d}_k = 1$ and the convergence error of the couple $\{\lambda_k(\theta), \mathbf{d}_k\}$ is defined as

$$\varepsilon_{\mathrm{local},j} = \left| \frac{\mathbb{E}\left\{\left(\lambda_{k,j}(\theta)\,\mathbf{d}_{k,j}\right)^2 - \left(\lambda_{k,j-1}(\theta)\,\mathbf{d}_{k,j-1}\right)^2\right\}}{\mathbb{E}\left\{\left(\lambda_{k,j}(\theta)\,\mathbf{d}_{k,j}\right)^2\right\}} \right| = \left| 1 - \frac{\mathbb{E}\left\{\lambda_{k,j-1}^2(\theta)\right\}}{\mathbb{E}\left\{\lambda_{k,j}^2(\theta)\right\}} \right|, \tag{9}$$

which measures the difference between $\lambda_{k,j}(\theta)$ and $\lambda_{k,j-1}(\theta)$. The calculation is stopped when $\lambda_{k,j}(\theta)$ is almost same as $\lambda_{k,j-1}(\theta)$. Also, the stop criterion of number k retained in the stochastic solution $\mathbf{u}(\theta)$ is defined as

$$\varepsilon_{\mathrm{global},k} = \left| \frac{\mathbb{E}\left\{\mathbf{u}_k^2(\theta) - \mathbf{u}_{k-1}^2(\theta)\right\}}{\mathbb{E}\left\{\mathbf{u}_k^2(\theta)\right\}} \right| = \left| 1 - \frac{\sum_{i,j=1}^{k-1} \mathbb{E}\left\{\lambda_i(\theta)\,\lambda_j(\theta)\right\} \mathbf{d}_i^{\mathrm{T}}\mathbf{d}_j}{\sum_{i,j=1}^{k} \mathbb{E}\left\{\lambda_i(\theta)\,\lambda_j(\theta)\right\} \mathbf{d}_i^{\mathrm{T}}\mathbf{d}_j} \right|. \tag{10}$$

In most problems, the stochastic global stiffness matrix $\mathbf{K}(\theta)$ and stochastic global load vector $\mathbf{F}(\theta)$ in stochastic finite element equation (4) are obtained by assembling stochastic element stiffness matrices and stochastic element load vector. They usually have the forms

$$\mathbf{K}(\theta) = \sum_{i=0}^{m} \xi_i(\theta)\,\mathbf{K}_i, \quad \mathbf{F}(\theta) = \sum_{i=0}^{q} \eta_i(\theta)\,\mathbf{F}_i, \tag{11}$$

where $\{\xi_i(\theta)\}_{i=1}^m$ and $\{\eta_i(\theta)\}_{i=1}^q$ are expanded random variables, $\{\mathbf{K}_i\}_{i=1}^m \in \mathbb{R}^{n\times n}$ and $\{\mathbf{F}_i\}_{i=1}^q \in \mathbb{R}^n$ are corresponding deterministic matrices and vectors, respectively, the random variables $\xi_0(\theta) = \eta_0(\theta) \equiv 1$, $\mathbf{K}_0 \in \mathbb{R}^{n\times n}$ and $\mathbf{F}_0 \in \mathbb{R}^n$ are the deterministic matrix and vector corresponding to the deterministic parts of material and load uncertainties. Eq. (11) provides a separated form of random variables and deterministic matrices. It is noted that random fields associated with material and load uncertainties do not have Eq. (11)-like separable forms in some cases. For non-separable random fields, series expansion methods, e.g., Karhunen–Loève expansion and Polynomial Chaos expansion, can be used to reformulate non-separable random fields as separable forms. Based on Eq. (11), Eq. (7) can be simplified and rewritten as

$$\widetilde{\mathbf{K}}_{kk}\mathbf{d}_k = \sum_{j=0}^{q} h_{jk}\mathbf{F}_j - \sum_{i=1}^{k-1} \widetilde{\mathbf{K}}_{ik}\mathbf{d}_i, \tag{12}$$

where deterministic matrices $\widetilde{\mathbf{K}}_{ij}$ are given by

$$\widetilde{\mathbf{K}}_{ij} = \sum_{l=0}^{m} c_{lij}\mathbf{K}_l, \tag{13}$$

where deterministic coefficients c_{ijk} and h_{ij} are computed by

$$c_{ijk} = \mathbb{E}\left\{\xi_i(\theta)\lambda_j(\theta)\lambda_k(\theta)\right\}, \quad h_{ij} = \mathbb{E}\left\{\eta_i(\theta)\lambda_j(\theta)\right\}. \tag{14}$$

The size of $\widetilde{\mathbf{K}}_{ij}$ in Eq. (13) is the same as the original stochastic finite element equation (4), which can be solved by existing deterministic FEM solvers [35, 36], thus it is readily applied to large-scale stochastic problems. Similarly, Eq. (8) can be simplified and rewritten as

$$a_k(\theta)\lambda_k(\theta) = b_k(\theta), \tag{15}$$

where random variables $a_k(\theta)$ and $b_k(\theta)$ are given by

$$a_k(\theta) = \sum_{i=0}^{m} g_{kik}\xi_l(\theta), \quad b_k(\theta) = \sum_{j=0}^{q} f_{kj}\eta_j(\theta) - \sum_{i=1}^{k-1}\sum_{j=0}^{m} g_{kji}\xi_j(\theta)\lambda_i(\theta) \tag{16}$$

where deterministic coefficients g_{ijk} and f_{ij} are calculated by

$$g_{ijk} = \mathbf{d}_i^{\mathrm{T}}\mathbf{K}_j\mathbf{d}_k, \quad f_{ij} = \mathbf{d}_i^{\mathrm{T}}\mathbf{F}_j. \tag{17}$$

Common methods solving Eq. (15) are to represent the random variable $\lambda_k(\theta)$ in terms of a set of polynomial chaos basis, but they have expensive computational costs [29, 31]. In order to avoid this difficulty, a sample-based method is developed to determine $\lambda_k(\theta)$. For sample realizations $\{\theta^{(i)}\}_{i=1}^{n_s}$ of all considered random event θ, sample realizations of the random variables $a_k(\theta)$ and $b_k(\theta)$ are calculated via

$$a_k\left(\widehat{\boldsymbol{\theta}}\right) = \xi\left(\widehat{\boldsymbol{\theta}}\right)\mathbf{g}_{k,\cdot,k}, \quad b_k\left(\widehat{\boldsymbol{\theta}}\right) = \eta\left(\widehat{\boldsymbol{\theta}}\right)\mathbf{f}_k - \left[\xi\left(\widehat{\boldsymbol{\theta}}\right)\mathbf{g}_{k,\cdot,1:k-1} \odot \lambda^{(k-1)}\left(\widehat{\boldsymbol{\theta}}\right)\right][\mathbf{1}]_{(k-1)\times 1}, \tag{18}$$

where $a_k\left(\widehat{\boldsymbol{\theta}}\right), b_k\left(\widehat{\boldsymbol{\theta}}\right) \in \mathbb{R}^{n_s}$ are the random sample vectors of the random variables $a_k(\theta)$ and $b_k(\theta)$, n_s is the number of sample realizations, the operator $\odot$ represents element-by-element multiplication of $\xi\left(\widehat{\boldsymbol{\theta}}\right)\mathbf{g}_{k,\cdot,1:k-1} \in \mathbb{R}^{n_s}$ and $\lambda^{(k-1)}\left(\widehat{\boldsymbol{\theta}}\right) \in \mathbb{R}^{n_s}$. The sample matrices of random variables $\{\xi_i(\theta)\}_{i=0}^{m}$, $\{\eta_i(\theta)\}_{i=0}^{q}$, $\{\lambda_i(\theta)\}_{i=1}^{k-1}$ are given by

$$\xi\left(\widehat{\boldsymbol{\theta}}\right) = \begin{bmatrix} 1 & \xi_1\left(\theta^{(1)}\right) & \cdots & \xi_m\left(\theta^{(1)}\right) \\ \vdots & \vdots & \ddots & \vdots \\ 1 & \xi_1\left(\theta^{(n_s)}\right) & \cdots & \xi_m\left(\theta^{(n_s)}\right) \end{bmatrix} \in \mathbb{R}^{n_s\times(m+1)}, \tag{19}$$

$$\eta\left(\widehat{\boldsymbol{\theta}}\right) = \begin{bmatrix} 1 & \eta_1\left(\theta^{(1)}\right) & \cdots & \eta_q\left(\theta^{(1)}\right) \\ \vdots & \vdots & \ddots & \vdots \\ 1 & \eta_1\left(\theta^{(n_s)}\right) & \cdots & \eta_q\left(\theta^{(n_s)}\right) \end{bmatrix} \in \mathbb{R}^{n_s\times(q+1)}, \tag{20}$$

$$\lambda^{(k-1)}\left(\widehat{\boldsymbol{\theta}}\right) = \begin{bmatrix} \lambda_1\left(\theta^{(1)}\right) & \cdots & \lambda_{k-1}\left(\theta^{(1)}\right) \\ \vdots & \ddots & \vdots \\ \lambda_1\left(\theta^{(n_s)}\right) & \cdots & \lambda_{k-1}\left(\theta^{(n_s)}\right) \end{bmatrix} \in \mathbb{R}^{n_s \times (k-1)} \tag{21}$$

and the coefficient matrices are given by

$$\mathbf{g}_k = \left[g_{kij}\right]_{ij} \in \mathbb{R}^{(m+1)\times k}, \quad \mathbf{f}_k = \left[f_{km}\right]_m \in \mathbb{R}^{q+1}, \tag{22}$$

where $\mathbf{g}_{k,\cdot,k} \in \mathbb{R}^{m+1}$ represents the k-th column of the matrix $\mathbf{g}_k$ and $\mathbf{g}_{k,\cdot,1:k-1} \in \mathbb{R}^{(m+1)\times k-1}$ represents columns 1 to $k-1$ of the matrix $\mathbf{g}_k$. With the sample realization vectors $a_k\left(\widehat{\boldsymbol{\theta}}\right)$ and $b_k\left(\widehat{\boldsymbol{\theta}}\right)$, the sample realization vector $\lambda_k\left(\widehat{\boldsymbol{\theta}}\right)$ of the random variable $\lambda_k(\theta)$ can be obtained by

$$\lambda_k\left(\widehat{\boldsymbol{\theta}}\right) = a_k\left(\widehat{\boldsymbol{\theta}}\right) \oslash b_k\left(\widehat{\boldsymbol{\theta}}\right) \in \mathbb{R}^{n_s}, \tag{23}$$

where the operator $\oslash$ denotes the element-wise division of two vectors, which can be performed cheaply even for a very large sample size n_s.

Statistical methods are then used to obtain probability characteristics of the random variable $\lambda_k(\theta)$ from random sample realizations $\lambda_k\left(\widehat{\boldsymbol{\theta}}\right) \in \mathbb{R}^{n_s}$. The computational cost for solving Eq. (23) is mainly concentrated on the calculation of the sample vectors $a_k\left(\widehat{\boldsymbol{\theta}}\right)$ and $b_k\left(\widehat{\boldsymbol{\theta}}\right)$ in Eq. (18). It is very low even for very high-dimensional stochastic problems since Eq. (18) is insensitive to the stochastic dimensionalities of $\xi(\theta)$ and $\eta(\theta)$. Specifically, even for very large numbers m and q (corresponding to the dimensionalities of $\xi(\theta)$ and $\eta(\theta)$), we can efficiently generate the sample realization matrices $\xi\left(\widehat{\boldsymbol{\theta}}\right)$ and $\eta\left(\widehat{\boldsymbol{\theta}}\right)$ via Eq. (19) and Eq. (20), and only matrix multiplication is involved in calculating the sample vectors $a_k\left(\widehat{\boldsymbol{\theta}}\right)$ and $b_k\left(\widehat{\boldsymbol{\theta}}\right)$ in Eq. (18), which is insensitive to stochastic dimensionalities and very cheap to calculate and store. In this way, high-dimensional stochastic spaces are cheaply and efficiently described and embedded into the random sample vectors $a_k\left(\widehat{\boldsymbol{\theta}}\right)$ and $b_k\left(\widehat{\boldsymbol{\theta}}\right)$. Furthermore, the proposed method combines the high efficiency of intrusive methods and the weak dependency on the dimensionality of non-intrusive methods. It is considered as a weakly intrusive approach. On one hand, Eq. (12) is fully deterministic and can be efficiently solved independently of the uncertainty, which is similar to intrusive approaches. On another hand, Eq. (23) is independent of the spatial position (or the finite element discretization) and solved only using random sample realizations, which is a non-intrusive way. In this sense, the proposed method avoids the curse of dimensionality to a great extent and is particularly appropriate for high-dimensional and large-scale stochastic problems in practice.

4. Reliability analysis using SFEM

We recall Eq. (3) and solve the stochastic solution vector $\mathbf{u}(\theta)$ of stochastic systems by use of the SFEM given in Section 3. Considering the stochastic displacement $\mathbf{u}(\theta) = \sum_{i=1}^{k} \lambda_i(\theta)\,\mathbf{d}_i$ and substituting it into Eq. (3) yield

$$g(\mathbf{x}, \theta) = g\left[h\left(\sum_{i=1}^{k} \lambda_i(\theta)\,\mathbf{d}_i\right), \mathbf{x}, \theta\right], \tag{24}$$

where the random parameters of the system are integrated into the random variables $\{\lambda_i(\theta)\}_{i=1}^{k}$ and the spatial parameter $\mathbf{x}$ is discretized and embedded into the deterministic vectors $\{\mathbf{d}_i\}_{i=1}^{k}$. Thus, the failure probability function $P_f(\mathbf{x})$ in Eq. (2) can be rewritten as

$$P_f(\mathbf{x}) = \Pr\left\{g\left[h\left(\sum_{i=1}^{k} \lambda_i(\theta)\,\mathbf{d}_i\right), \mathbf{x}, \theta\right] \leq 0\right\}. \tag{25}$$

It is noted that the proposed method strongly depends on the applicability of the proposed SFEM. The reliability analysis for nonlinear stochastic problems is the same as mentioned above but based on solutions of nonlinear stochastic finite element equations. The most straightforward and efficient way to compute Eq. (25) is MCS. Random samples used in MCS are generated according to the distribution of θ, and the numbers of the points landing in the failure domain are counted to estimate the failure probability. Similar to the process of MCS, we utilize a sample-based method to estimate Eq. (25). Random sample realizations $\left\{\lambda_i\left(\theta^{(j)}\right)\right\}_{j=1}^{n_s}$, $i = 1, \cdots, k$ in Eq. (25) have been calculated by use of Eq. (23), thus the failure probability function $P_f(\mathbf{x})$ can be evaluated in the following form

$$P_f(\mathbf{x}) = \frac{1}{n_s} \sum_{j=1}^{n_s} \mathcal{I}\left\{g\left[h\left(\sum_{i=1}^{k} \lambda_i\left(\theta^{(j)}\right)\mathbf{d}_i\right), \mathbf{x}, \theta^{(j)}\right]\right\}, \tag{26}$$

where $\mathcal{I}(\cdot)$ is the indicator function satisfying

$$\mathcal{I}(s) = \begin{cases} 1, & s \leq 0 \\ 0, & s > 0 \end{cases}. \tag{27}$$

The proposed method in Eq. (26) combines the high accuracy of sampling methods and the high efficiency of non-sampling methods. On one hand, as a sample-based method, it has comparable accuracy with the Monte Carlo method. The accuracy increases as the number of samples increases. On the other hand, it does not require a full-scale simulation of the underlying system for each sample realization and only depends on the stochastic solution obtained by the proposed SFEM. Specifically, the full-scale deterministic finite element equation is solved for each sample realization if classical sampling-type methods are used. The number of finite element equations to solve is equal to the number of sample realizations. While the proposed method only requires solving a few numbers of Eq. (12) (or Eq. (7)) and Eq. (23). The number usually weakly depends on the number of sample realizations. The computational efficiency is thus greatly improved since fewer equations are solved. In addition, Eq. (26) can compute the failure probability $P_f(\mathbf{x}_i)$ for each spatial position $\mathbf{x}_i$ at once, which provides a simple but effective way to identify multiple failure modes of complex systems. Hence, the proposed method provides a unified framework for reliability analysis. It is particularly appropriate for high-dimensional and complex stochastic problems in practice.

5. Algorithm implementation

The resulting procedure for solving the stochastic finite element equation (4) and computing the failure probability function $P_f(\mathbf{x})$ via Eq. (26) are summarized in Algorithm 1, which includes two parts in turn. The first part is from step 2 to step 9, which is to compute the stochastic displacement $\mathbf{u}(\theta)$ and includes a double-loop iteration procedure. The inner loop, which is from step 4 to step 7, is used to determine the couple $\{\lambda_k(\theta), \mathbf{d}_k\}$. While the outer loop, which is from step 2 to step 9, corresponds to recursively building the set of couples such that the approximate solution $\mathbf{u}(\theta)$ satisfies Eq. (4). In step 2 and step 7, iterative errors $\varepsilon_{\text{global},k}$ and $\varepsilon_{\text{local},j}$ are calculated via Eq. (10) and Eq. (9) and corresponding convergence errors ε_1 and ε_2 are specified precisions. It is noted that the initializations in step 1 and step 3 have little influence on the computational accuracy and efficiency of the proposed method. In practical implementation, any nonzero vectors of size n_s can be adopted as the initial random samples. The second part consists of step 10 and step 11, where the spatial limit state function $g(\mathbf{x}, \theta)$ in step 10 is generated based on the stochastic displacement $\mathbf{u}(\theta)$ obtained in step 8, and the spatial failure probability function $P_f(\mathbf{x})$ is calculated in step 11.

Algorithm 1 Reliability analysis based on SFEM

1: Initialize random samples $\xi_i\left(\widehat{\boldsymbol{\theta}}\right) \in \mathbb{R}^{n_s}$, $i = 1, \cdots, m$ and $\eta_i\left(\widehat{\boldsymbol{\theta}}\right) \in \mathbb{R}^{n_s}$, $i = 1, \cdots, q$

2: **while** $\varepsilon_{\text{global},k} > \varepsilon_1$ **do**

3:     Initialize samples $\lambda_{k,0}\left(\widehat{\boldsymbol{\theta}}\right) \in \mathbb{R}^{n_s}$ of the random variable $\lambda_{k,0}(\theta)$

4:     **repeat**

5:         Compute the displacement component $\mathbf{d}_{k,j}$ by solving Eq. (12)

6:         Compute the random samples $\lambda_{k,j}\left(\widehat{\boldsymbol{\theta}}\right) \in \mathbb{R}^{n_s}$ via Eq. (23)

7:     **until** $\varepsilon_{\text{local},j} < \varepsilon_2$

8:     $\mathbf{u}_k(\theta) = \sum\limits_{i=1}^{k-1} \lambda_i(\theta)\,\mathbf{d}_i + \lambda_k(\theta)\,\mathbf{d}_k,\ k \geq 2$

9: **end while**

10: Compute the spatial limit state function $g(\mathbf{x}, \theta)$ via Eq. (24)

11: Compute the spatial failure probability function $P_f(\mathbf{x})$ via Eq. (26)

---

6. Numerical examples

In this section, we present three examples to illustrate the high accuracy and high efficiency of the proposed method in comparison to existing methods, including the reliability analysis of a beam-bar frame, the reliability analysis of a roof truss defined in 100-dimensional stochastic spaces and the global reliability analysis of a plate. For all considered examples, 1×10^6 initial samples $\left\{\xi_i\left(\theta^{(j)}\right)\right\}_{j=1}^{1\times10^6}$, $\left\{\eta_i\left(\theta^{(j)}\right)\right\}_{j=1}^{1\times10^6}$ and $\left\{\lambda_{k,0}\left(\theta^{(j)}\right)\right\}_{j=1}^{1\times10^6}$ of random variables $\xi_i(\theta)$, $\eta_i(\theta)$ and $\lambda_{k,0}(\theta)$ are given and the convergence errors in step 2 and step 7 of Algorithm 1 are set as $\varepsilon_1 = 1 \times 10^{-5}$ and $\varepsilon_2 = 1 \times 10^{-3}$, respectively.

6.1. Reliability analysis of a beam-bar frame

A two-layer frame consists of horizontal and vertical beams and is stabilized with diagonal bars, as shown in Fig. 1. Probability distributions of independent random variables associated

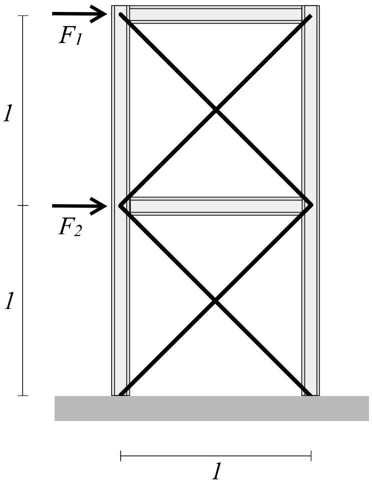

Figure 1: Model of the two-layer frame.

with material properties, geometry properties and loads are listed in Table 1. In this example, we consider the failure probability of a single point and the limit state function $g(\theta)$ is given by the maximum joint displacement of the frame as

$$g(\theta) = \max_i \sqrt{u_{x_i}^2 + u_{y_i}^2} - c \cdot u_{mean}, \tag{28}$$

where $u_{mean} = \text{mean}\left(\max_i \sqrt{u_{x_i}^2(\theta) + u_{y_i}^2(\theta)}\right)$ is the mean value of the maximum joint displacement and the scalar c is related to different failure probabilities, that is, the failure probability decreases

Table 1: Probability distributions of random variables in the Example 6.1.

variable	description	distribution	mean	variance
E_{beam}	Young's modulus of beam	normal	210 MPa	0.2
A_{beam}	cross-sectional area of beam	lognormal	100 mm^2	0.2
I_{beam}	moment of inertia of beam	lognormal	800 mm^4	0.2
E_{bar}	Young's modulus of bar	normal	210 MPa	0.2
A_{bar}	cross-sectional area of bar	lognormal	100 mm^2	0.2
F_1, F_2	load 1 and 2	normal	10 kN	0.2

as the scalar c increases. By use of the proposed method, the maximum joint displacement of the frame can be identified automatically instead of selecting manually since the proposed method can calculate the stochastic displacements of all nodes simultaneously.

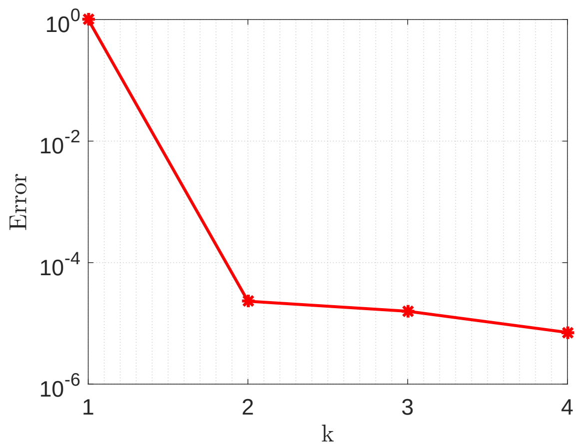

Figure 2: Iteration errors of different retained items.

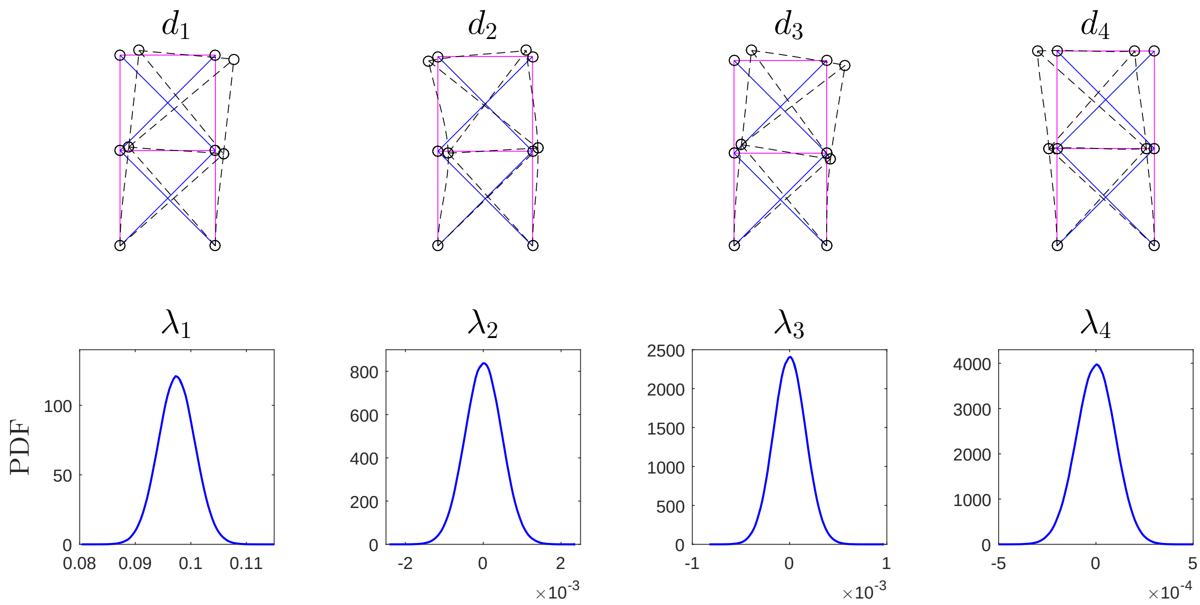

Figure 3: Solutions of the couples $\{\lambda_i(\theta), \mathbf{d}_i\}_{i=1}^{4}$.

In order to compute the failure probability P_f, we first compute the stochastic displacement of the frame by using the first part of Algorithm 1. The iterative errors of different retained terms calculated by Eq. (10) are shown in Fig. 2. It is seen that only four iterations achieve the required precision $\varepsilon_1 = 1 \times 10^{-5}$, which demonstrates the fast convergence rate of the proposed SFEM. Correspondingly, as shown in Fig. 3, the number of couples $\{\lambda_k(\theta), \mathbf{d}_k\}$ that constitute the stochastic displacement is adopted as $k = 4$. With the increasing the number of couples, the ranges of corresponding random variables are more closely approaching zero, which indicates that the contribution of the higher-order random variables to the approximate stochastic solution decays dramatically.

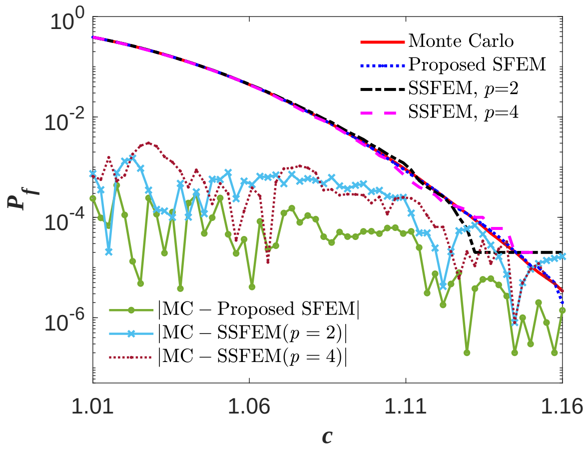

Figure 4: Failure probabilities of different scalar c.

Based on the stochastic displacement obtained by SFEM, failure probabilities of different scalar c are shown in Fig. 4, where the scalar c is set from 1.01 to 1.16. The failure probability P_f computed from the proposed method ranges from 10^0 to 10^{-6}, which is fairly close to that obtained from 1×10^6 MCS even for a very small failure probability. The absolute error between the proposed method and MCS demonstrates the high accuracy of the proposed method. As a comparison, we compute the stochastic displacement by SSFEM [26, 31]. The Hermite PC basis of seven standard Gaussian random variables are chosen to expand the stochastic displacement, and the order of Hermite PC basis is set as $p = 2$ and $p = 4$, respectively. For the order $p = 2$ and $p = 4$, the sizes of deterministic finite element equations derived from SSFEM are 423 and 3960, respectively. We test the computational efficiencies of these methods by use of a personal laptop (dual-core, Intel Core i7, 2.40GHz). The CPU times of the proposed method, SSFEM ($p = 2$), SSFEM ($p = 4$) and 1×10^6 MCS are 3.18s, 16.05s, 84.66s and 374.71s, respectively, which demonstrates the high efficiency of the proposed method. Failure probabilities based on SSFEM and corresponding absolute errors referring to MCS are shown in Fig. 4, which indicates that SSFEM ($p = 4$) is more accurate than SSFEM ($p = 2$). The proposed method has a smaller absolute error than SSFEM, especially for small failure probabilities. SSFEM has poor accuracy when the failure probability is less than 10^{-4} and cannot capture the failure probability less than 10^{-5}, while the proposed method has a good accuracy even for the failure probability close to 10^{-6}, which demonstrates the high accuracy of the proposed method.

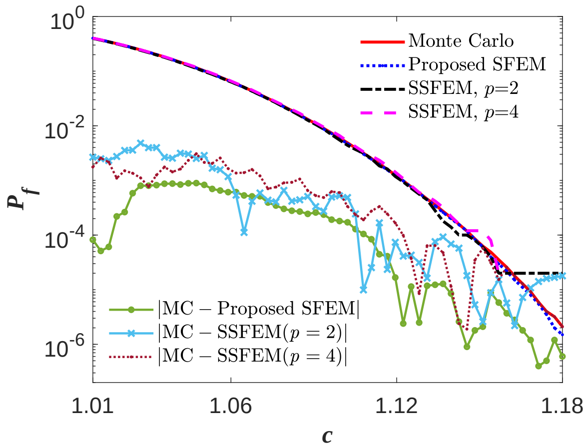

Figure 5: Failure probabilities of different scalar c.

Furthermore, we consider the frame working in an elastic state, and the limit state function is associated with the ultimate interlayer shear force $c \cdot \overline{\sigma}_s$, where c is a scale factor and $\overline{\sigma}_s$ is the mean interlayer shear force. The maximum interlayer shear force is computed by the proposed method, SSFEM and 1×10^6 MCS, respectively. Fig. 5 shows failure probabilities obtained by these methods and corresponding absolute errors referring to MCS. Similar to that in Fig. 4, both SSFEM ($p = 2$) and SSFEM ($p = 4$) have poor accuracy for small failure probabilities, while the proposed method is fairly close to the results obtained by MCS. The proposed method still achieves good accuracy in this case.

6.2. Reliability analysis of a roof truss

In this example, we consider that a stochastic wind load acts vertically downward on a roof truss [32], as shown in Fig. 6. The roof truss includes 185 spatial nodes and 664 elements and material properties of all members are set as Young's modulus $E = 209\text{GPa}$ and cross-sectional areas $A = 16\text{cm}^2$. The stochastic wind load $f(x, y, \theta)$ is a random field with the covariance function $C_{ff}(x_1, y_1; x_2, y_2) = \sigma_f^2 e^{-|x_1-x_2|/l_x - |y_1-y_2|/l_y}$, where the variance $\sigma_f^2 = 1.2$, the correlation lengths $l_x = l_y = 24$. It can be expanded by use of Karhunen-Loève expansion [33, 34, 37] with M-term truncated

$$f(x, y, \theta) = \sum_{i=0}^{M} \xi_i(\theta) \sqrt{\nu_i} f_i(x, y), \tag{29}$$

where $\nu_0 = \xi_0(\theta) \equiv 1$, the mean function $f_0(x, y) = 10\text{kN}$, $\{\xi_i(\theta)\}_{i=1}^M$ are uncorrelated standard Gaussian random variables, ν_i and $f_i(x, y)$ are eigenvalues and eigenfunctions of the covariance function $C_{ff}(x_1, y_1; x_2, y_2)$, which can be obtained by solving an eigen equation [38].

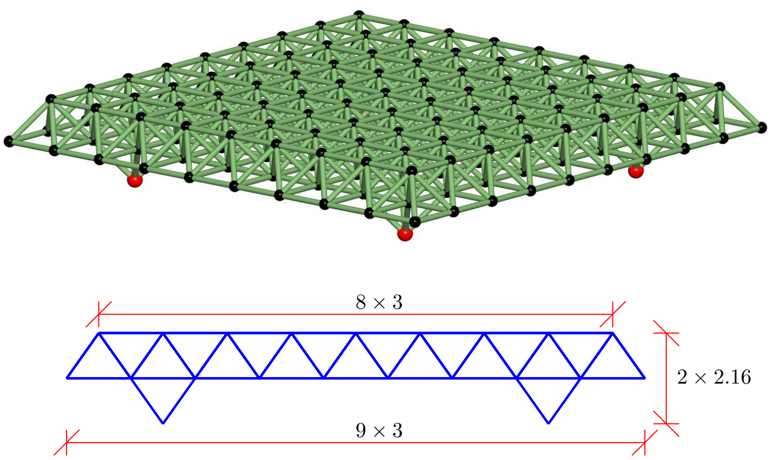

Figure 6: Model of the roof truss.

Similar to Example 6.1, we consider the failure probability of the maximum displacement of the roof truss and the limit state function $g(\theta)$ is defined by the maximum displacement as

$$g(\theta) = \max_i u_i(\theta) - c \cdot u_{mean}, \tag{30}$$

where $u_{mean} = \text{mean}\left(\max\limits_i u_i(\theta)\right)$ is the mean value of the maximum displacement, $u_i(\theta)$ are vertical displacements of all spatial nodes and the scalar c is related to different failure probabilities.

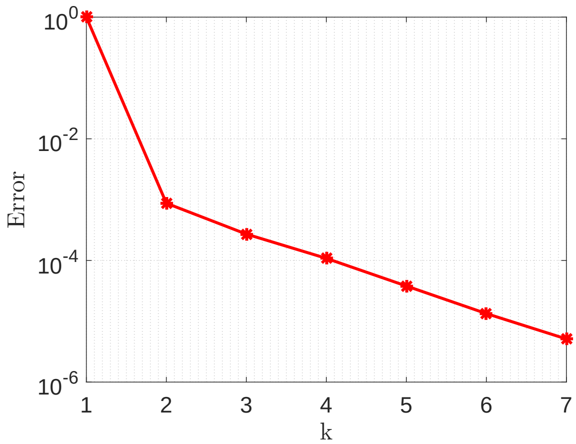

Figure 7: Iteration errors of different retained items.

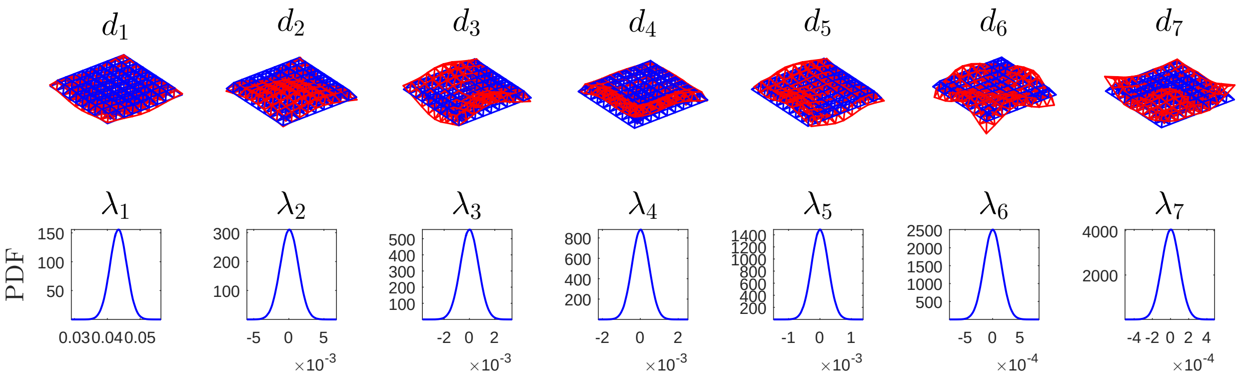

Figure 8: Solutions of the couples $\{\lambda_i(\theta), \mathbf{d}_i\}_{i=1}^{7}$.

A stochastic finite element equation of the stochastic displacement $\mathbf{u}(\theta)$ is obtained based on the expansion (29) of the stochastic wind load. In order to verify the effectiveness of the proposed method for high-dimensional reliability analysis, we adopt the stochastic dimension $M = 100$ in Eq. (29). The iterative errors of different retained terms calculated by Eq. (10) are shown in Fig. 7. Seven iterations can achieve the required precision $\varepsilon_1 = 1 \times 10^{-5}$, which indicates the fast convergence rate of the proposed method even for very high stochastic dimensions. The deterministic displacement components $\{\mathbf{d}_i\}_{i=1}^{7}$ and PDFs of corresponding random variables $\{\lambda_i(\theta)\}_{i=1}^{7}$ are shown in Fig. 8. The computational time for calculating couples $\{\lambda_i(\theta), \mathbf{d}_i\}_{i=1}^{7}$ in this example is 21.90s by use of a personal laptop (dual-core, Intel Core i7, 2.40GHz), while 854.47s are used for MCS, which indicates that Algorithm 1 still has less computational costs for high-dimensional stochastic problems. The resulting approximate probability density function (PDF) of the maximum stochastic displacement of the whole roof truss compared with that obtained by 1×10^6 MCS is seen from Fig. 9, which indicates that the result of seven-term approximation is in very good accordance with that from MCS. Further increasing the number of couples will not significantly improve the accuracy since the series in Eq. (5) has converged. It is noted that the tail of the probability distribution is crucial for reliability analysis. The proposed method is based on random samples and it can provide a good approximation for the tail of the probability distribution.

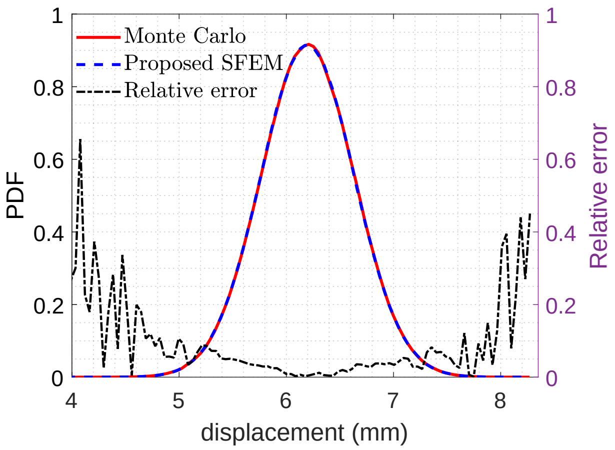

Figure 9: PDFs of the maximum stochastic displacement obtained by MCS and the proposed method and their relative error.

In this example, the scalar parameter c in Eq. (30) is set from 1.10 to 1.31 and failure probabilities of different scalar c are shown in Fig. 10. The computational accuracy of the proposed method is verified again in comparison to 1×10^6 MCS. The accuracy of the proposed method decreases when the failure probability P_f is close to 10^{-6}, but it still has a good match with the result from MCS. The high-dimensional reliability analysis in this example is performed with low computational costs, thus the curse of dimensionality encountered in high-dimensional stochastic spaces is thus overcome successfully.

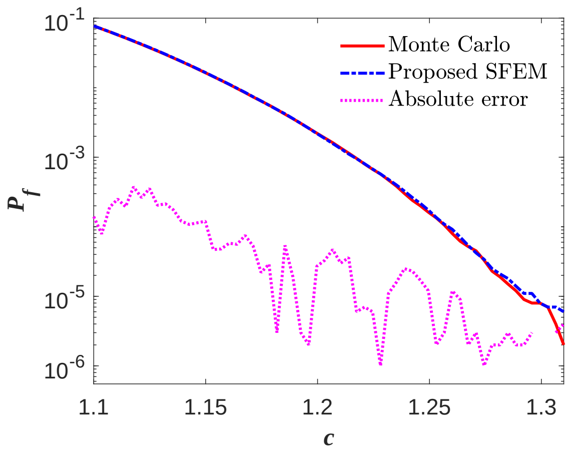

Figure 10: Failure probabilities of different scalar c.

6.3. Global reliability analysis of a plate

In this example, we consider a Kirchhoff-Love thin plate subjected to a deterministic distributed load $q = -10\mathrm{kN}\big/\mathrm{m}^2$ and simply supported on four edges. As shown in Fig. 11, parameters of this problem are set as length $L = 4$m, width $D = 2$m, thickness $t = 0.05$m and Poisson's ratio $\nu = 0.3$. For the sake of simplicity, we neglect the self-weight of the plate and assume Young's modulus $E(x, y, \theta)$ as the realization of a Gaussian random field with the mean function $\mu_E = 210$GPa and the covariance function $C_{EE}(x_1, y_1; x_2, y_2) = \sigma_E^2 e^{-|x_1-x_2|/l_x - |y_1-y_2|\big/l_y}$, where the

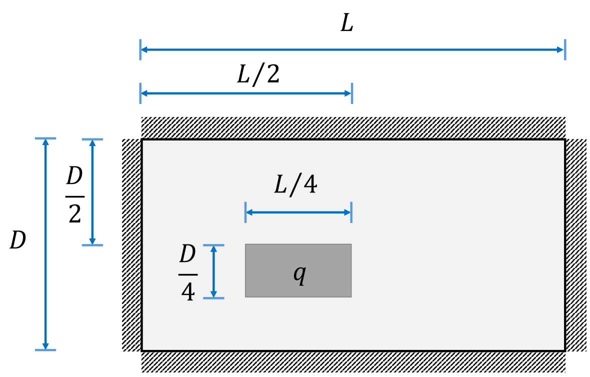

Figure 11: Model of the plate.

correlation lengths $l_x = 2\text{m}$, $l_y = 4\text{m}$, the standard deviation $\sigma_E = 22\text{GPa}$. Similar to Eq. (29), Young's modulus $E(x, y, \theta)$ is approximated by Karhunen-Loève expansion with the 10-term truncation

$$E(x, y, \theta) = \mu_E + \sum_{i=1}^{10} \xi_i(\theta) E_i(x, y). \tag{31}$$

In this example, we consider failure probabilities of all spatial points, which can be considered as a global reliability analysis. The global limit state function $g(\mathbf{x}, \theta)$ is defined by the stochastic displacement of the plate exceeding a critical threshold as

$$g(\mathbf{x}, \theta) = u_\omega(\mathbf{x}, \theta) - c \cdot u_{\omega,mean}(\mathbf{x}), \tag{32}$$

where $u_\omega(\mathbf{x}, \theta)$ is the vertical stochastic displacement field of all spatial nodes, $u_{\omega,mean}(\mathbf{x}) = \text{mean}(u_\omega(\mathbf{x}, \theta))$ is the corresponding mean displacement field of $u_\omega(\mathbf{x}, \theta)$ and the scalar parameter is set as $c = 1.35$.

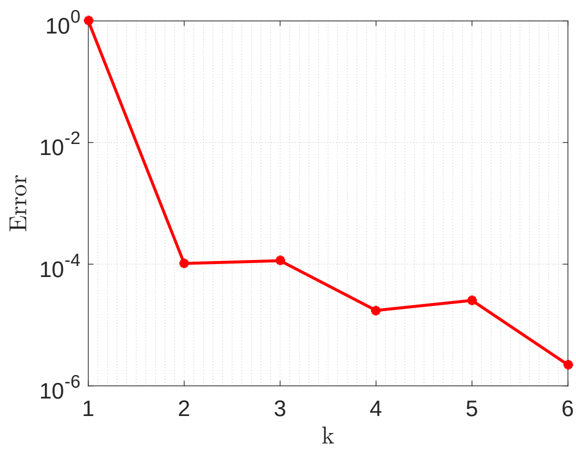

Figure 12: Iteration errors of different retained items.

We adopt the Kirchhoff-Love theory and four-node finite elements to divide the plate into 861 nodes and 800 elements. The unknown node displacement $\mathbf{u}(\theta)$ is introduced as $\mathbf{u}(\theta) = [\mathbf{u}_\omega(\theta), \mathbf{u}_x(\theta), \mathbf{u}_y(\theta)]^{\mathrm{T}}$, which are the vertical displacement, rotations in x and y axes, respectively. 2583 degrees of freedom are thus defined. The iterative errors of different retained terms calculated by Eq. (10) are found in Fig. 12. The required precision $\varepsilon_1 = 1 \times 10^{-5}$ can be achieved after six iterations. Fig. 13 shows the vertical displacement components $\{\mathbf{d}_i\}_{i=1}^{6}$ and PDFs of corresponding random variables $\{\lambda_i(\theta)\}_{i=1}^{6}$, which again indicates that the first few couples dominate the stochastic solution even for very complex stochastic problems.

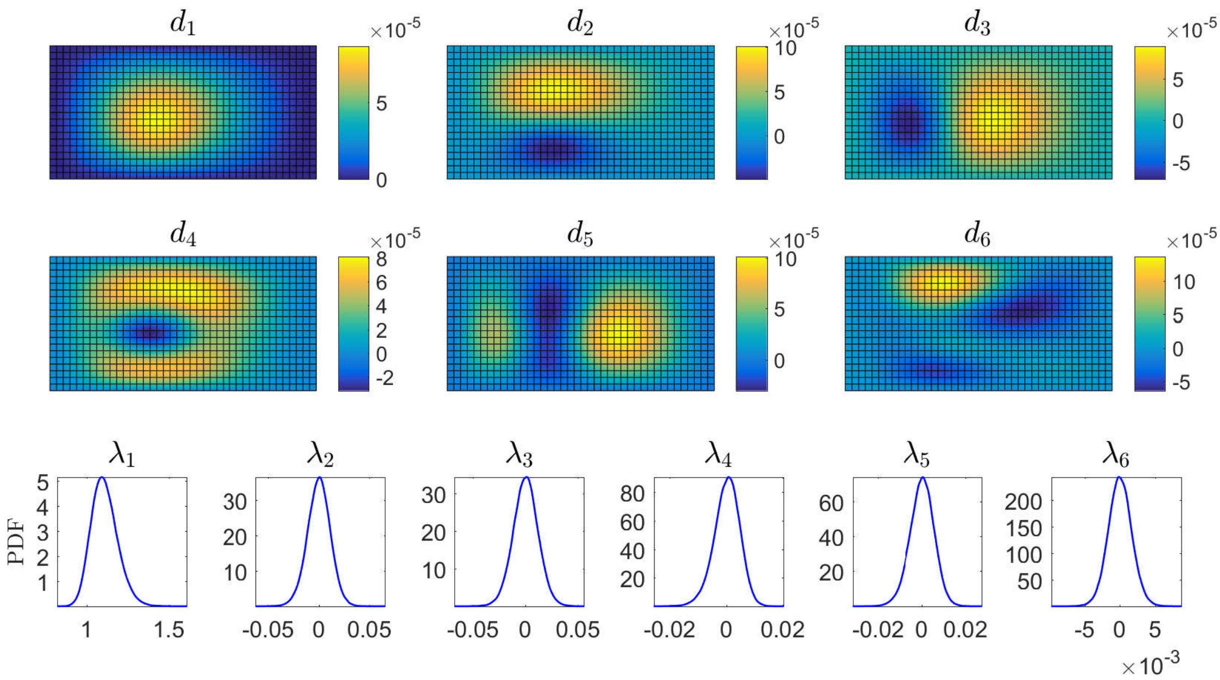

Figure 13: Solutions of the couples $\{\lambda_i(\theta), \mathbf{d}_i\}_{i=1}^{6}$.

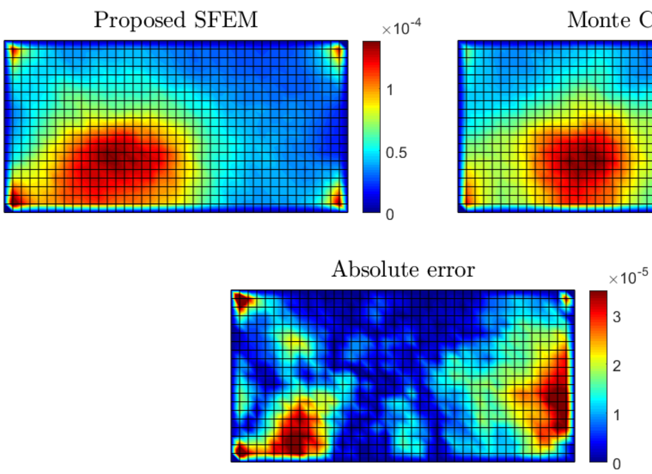

Figure 14: Failure probability nephogram.

Based on the vertical stochastic displacement $\mathbf{u}_{\omega}(\theta)$ obtained by the proposed SFEM, the global failure probability $P_f(\mathbf{x})$ of the plate can be calculated by use of Eq. (26) (i.e. the step 11 in Algorithm 1). As shown in Fig. 14, the failure probability nephogram has a good accordance with that from 1×10^6 MCS, which demonstrates the effectiveness and the high accuracy of the proposed method for global reliability analysis. It is noted that failure probabilities $P_f(\mathbf{x}_i)$ of all spatial nodes constitute the global failure probability $P_f(\mathbf{x})$ shown in Fig. 14, thus several difficulties encountered in existing approaches can be circumvented, such as determining the design point (a point lying on the failure surface which has the highest probability density among other points on the failure surface). In this way, the proposed method provides a novel strategy for global reliability analysis.

7. Conclusion

This paper presents an efficient and unified methodology for structural reliability analysis and illustrates its accuracy and efficiency using three numerical examples. The proposed method first calculates structural stochastic displacements by using an efficient stochastic finite element method, and the failure probability is subsequently calculated based on the obtained stochastic displacements. As shown in three considered examples, the proposed method has a same implementation process for different stochastic problems and allows to solve high-dimensional stochastic problems with low computational costs. The curse of dimensionality encountered in high-dimensional reliability analysis can thus be circumvented with great success. In addition, the proposed method achieves a high-precision solution of global reliability analysis, which overcomes difficulties encountered in existing approaches and provides a new strategy for the reliability analysis of complex stochastic problems. In these senses, the methodology proposed in this paper is particularly appropriate for large-scale and high-dimensional reliability analysis of practical interests and has great potential in reliability analysis in science and engineering. In the follow-up research, a wider range of reliability analyses will be further investigated, such as reliability analysis of time-dependent and nonlinear problems.

Acknowledgments

This research is supported by the China Postdoctoral Science Foundation (Project 2021M690839), the Research Foundation of Harbin Institute of Technology and the National Natural Science Foundation of China (Project 11972009). These supports are gratefully acknowledged.

References

[1] R. E. Melchers, A. T. Beck, Structural reliability analysis and prediction, John Wiley & Sons, 2018.

[2] P. Thoft-Cristensen, M. J. Baker, Structural reliability theory and its applications, Springer Science & Business Media, 2012.

[3] S. Mahadevan, P. Nath, Z. Hu, Uncertainty quantification for additive manufacturing process improvement: Recent advances, ASCE-ASME Journal of Risk and Uncertainty in Engineering Systems, Part B: Mechanical Engineering 8 (2022) 010801.

[4] P.-S. Koutsourelakis, H. Pradlwarter, G. Schuëller, Reliability of structures in high dimensions, part I: algorithms and applications, Probabilistic Engineering Mechanics 19 (2004) 409–417.

[5] S.-K. Au, J. L. Beck, A new adaptive importance sampling scheme for reliability calculations, Structural Safety 21 (1999) 135–158.

[6] M. Faes, J. Sadeghi, M. Broggi, M. De Angelis, E. Patelli, M. Beer, D. Moens, On the robust estimation of small failure probabilities for strong nonlinear models, ASCE-ASME Journal of Risk and Uncertainty in Engineering Systems, Part B: Mechanical Engineering 5 (2019).

[7] M. Papadrakakis, N. D. Lagaros, Reliability-based structural optimization using neural networks and Monte Carlo simulation, Computer Methods in Applied Mechanics and Engineering 191 (2002) 3491–3507.

[8] V. Dubourg, B. Sudret, J.-M. Bourinet, Reliability-based design optimization using kriging surrogates and subset simulation, Structural and Multidisciplinary Optimization 44 (2011) 673–690.

[9] S. K. Au, J. Ching, J. Beck, Application of subset simulation methods to reliability benchmark problems, Structural Safety 29 (2007) 183–193.

[10] A. Der Kiureghian, H.-Z. Lin, S.-J. Hwang, Second-order reliability approximations, Journal of Engineering Mechanics 113 (1987) 1208–1225.

[11] B. Sudret, A. Der Kiureghian, Stochastic finite elements and reliability: a state-of-the-art report, University of California, Berkeley (2000) 114–120.

[12] R. Rackwitz, Reliability analysis—a review and some perspectives, Structural Safety 23 (2001) 365–395.

[13] G. Schueller, H. Pradlwarter, P. Koutsourelakis, A critical appraisal of reliability estimation procedures for high dimensions, Probabilistic Engineering Mechanics 19 (2004) 463–474.

[14] H. P. Gavin, S. C. Yau, High-order limit state functions in the response surface method for structural reliability analysis, Structural Safety 30 (2008) 162–179.

[15] D. Li, Y. Chen, W. Lu, C. Zhou, Stochastic response surface method for reliability analysis of rock slopes involving correlated non-normal variables, Computers and Geotechnics 38 (2011) 58–68.

[16] Z. Zheng, P. Wang, Uncertainty quantification analysis on silicon electrodeposition process via numerical simulation methods, ASCE-ASME Journal of Risk and Uncertainty in Engineering Systems, Part B: Mechanical Engineering 8 (2022).

[17] L. Zhang, Z. Lu, P. Wang, Efficient structural reliability analysis method based on advanced Kriging model, Applied Mathematical Modelling 39 (2015) 781–793.

[18] Bourinet, J-M, Rare-event probability estimation with adaptive support vector regression surrogates., Reliability Engineering & System Safety (2016).

[19] R. Chowdhury, B. Rao, Hybrid high dimensional model representation for reliability analysis, Computer Methods in Applied Mechanics and Engineering 198 (2009) 753–765.

[20] J. Li, D. Xiu, Evaluation of failure probability via surrogate models, Journal of Computational Physics 229 (2010) 8966–8980.

[21] S. Marelli, B. Sudret, An active-learning algorithm that combines sparse polynomial chaos expansions and bootstrap for structural reliability analysis, Structural Safety 75 (2018) 67–74.

[22] K. Cheng, Z. Lu, Structural reliability analysis based on ensemble learning of surrogate models, Structural Safety 83 (2020) 101905.

[23] K. Zuev, Subset simulation method for rare event estimation: an introduction, Encyclopedia of Earthquake Engineering (2015).

[24] X. Zhang, M. D. Pandey, Structural reliability analysis based on the concepts of entropy, fractional moment and dimensional reduction method, Structural Safety 43 (2013) 28–40.

[25] X. Wang, Y. Liao, M. P. Mignolet, Uncertainty analysis of piezoelectric vibration energy harvesters using a finite element level-based maximum entropy approach, ASCE-ASME Journal of Risk and Uncertainty in Engineering Systems, Part B: Mechanical Engineering 7 (2021) 010906.

[26] R. G. Ghanem, P. D. Spanos, Stochastic finite elements: a spectral approach, Courier Corporation, 2003.

[27] D. Xiu, G. E. Karniadakis, The Wiener–Askey polynomial chaos for stochastic dierential equations, SIAM Journal on Scientific Computing 24 (2002) 619–644.

[28] H. G. Matthies, A. Keese, Galerkin methods for linear and nonlinear elliptic stochastic partial differential equations, Computer Methods in Applied Mechanics Engineering 194 (2005) 1295–1331.

[29] A. Nouy, Recent developments in spectral stochastic methods for the numerical solution of stochastic partial differential equations, Archives of Computational Methods in Engineering 16 (2009) 251–285.

[30] G. Stefanou, The stochastic finite element method: past, present and future, Computer Methods in Applied

Mechanics and Engineering 198 (2009) 1031–1051.

[31] D. Xiu, Numerical methods for stochastic computations: a spectral method approach, Princeton University Press, 2010.

[32] Z. Zheng, H. Dai, Structural stochastic responses determination via a sample-based stochastic finite element method, Computer Methods in Applied Mechanics and Engineering 381 (2021) 113824.

[33] K. Phoon, S. Huang, S. Quek, Simulation of second-order processes using Karhunen–Loève expansion, Computers & Structures 80 (2002) 1049–1060.

[34] Z. Zheng, H. Dai, Simulation of multi-dimensional random fields by Karhunen–Loève expansion, Computer Methods in Applied Mechanics and Engineering 324 (2017) 221–247.

[35] T. J. Hughes, The finite element method: linear static and dynamic finite element analysis, Courier Corporation, 2012.

[36] J. N. Reddy, An introduction to nonlinear finite element analysis: with applications to heat transfer, fluid mechanics, and solid mechanics, OUP Oxford, 2014.

[37] S. Rahman, A Galerkin isogeometric method for Karhunen-Loève approximation of random fields, Computer Methods in Applied Mechanics and Engineering 338 (2018) 533–561.

[38] S. M. Zemyan, The classical theory of integral equations: a concise treatment, Springer Science & Business Media, 2012.